

## Alignment of a Restriction Map with the Genetic Map of Bacteriophage T4

JIING KUAN YEE AND ROBERT C. MARSH\*

*Biology Program, University of Texas at Dallas, Richardson, Texas 75080*

Received 1 October 1980/Accepted 31 December 1980

A restriction map of the bacteriophage T4 genome was aligned with the T4 genetic map. Included were the cleavage sites for *Bam*HI, *Bgl*II, *Kpn*I, *Pvu*I, *Sal*I, and *Xba*I. The alignment utilized the fact that the T4 genetic map had been oriented previously with respect to a T2/T4 heteroduplex map. DNA fragments from a *Bgl*II digestion of cytosine-containing DNA from a T4 dCTPase<sup>-</sup> *denA denB*(rIIH23B) *alc* mutant were hybridized with full-length chromosomal strands of bacteriophage T2, and the heteroduplexes were examined by electron microscopy. From their lengths and patterns of substitution and deletion loops, the heteroduplexes formed with 6 of the 13 *Bgl*II fragments could be unambiguously identified and positioned on the T2/T4 heteroduplex map. The ends of the T4 DNA strands in the heteroduplexes directly identified the location of 10 *Bgl*II cleavage sites. The remaining three *Bgl*II cleavage sites could be assigned to the T2/T4 heteroduplex map based on their relative locations on the restriction map. It was also possible to identify the source of the DNA strands (i.e., T2 or T4) in four previously unassigned deletion loops on the T2/T4 heteroduplex. Among the *Bgl*II fragments identified in heteroduplexes was the fragment containing the rIIH23B deletion; this deletion was used as the primary point of reference for alignment of the T4 restriction map with the T2/T4 heteroduplex map and, hence, with the T4 genetic map.

Since the isolation of bacteriophage T4 mutants which allow the growth and packaging of DNA containing cytosine instead of the glucosylated hydroxymethylcytosine residues normally present (15), T4 DNA has been amenable to analysis with restriction endonucleases. Circular cleavage maps of the 166-kilobase pair T4 genome have been published for restriction enzymes *Bam*HI, *Bgl*II, *Kpn*I, *Sal*I, *Sma*I, and *Xho*I (3, 6, 14), and maps for *Bgl*I, *Eco*RI, *Hind*III, and *Pst*I have been completed recently (2, 12). In the accompanying report, the sites of cleavage by *Pvu*I and *Xba*I were added to a computer-fitted, unified map of the *Bam*HI, *Bgl*II, *Kpn*I, and *Sal*I cleavage sites (9). Altogether, more than 250 cleavage sites have been identified on the T4 genome.

We extend the usefulness of these maps by reporting here an alignment between our computer-fitted restriction map and the T4 genetic map. Heteroduplexes were formed between T4 *Bgl*II fragments and full-length T2 chromosomal strands and examined by electron microscopy. From the positions of the ends of the T4 strands relative to known T2/T4 nonhomologies, the *Bgl*II cleavage sites could be located on the T2/T4 heteroduplex map. This made possible an alignment between the restriction map

and the T4 genetic map, as the T2/T4 heteroduplex map had been oriented previously with respect to the T4 genetic map (7). The alignment of the restriction and genetic maps is fixed by the position of an rII deletion. The maps appear to be correlated within 1 to 2 kilobases (kb) over their entirety.

O'Farrell et al. (12) have independently aligned a T4 restriction map with the genetic map, primarily by filter hybridization of restriction fragments to cloned segments of T4 DNA known to carry specific genes. Also, Carlson (2) has determined a general alignment based on the cleavage patterns of cytosine-containing DNA from T4 *alc* mutants which carry various characterized deletions. Our results are in agreement.

### MATERIALS AND METHODS

**Phage and bacterial strains.** Bacteriophage T4 56<sup>-</sup> (*amE51* dCTPase<sup>-</sup> *denA*(nd28) *denB*(ΔrIIH23B) *alc8* and its restriction/modification-negative hosts *Escherichia coli* K803 (*supE hsdS rgl gal met*) and B834 (*supE*<sup>+</sup> *r<sub>B</sub>*<sup>-</sup> *m<sub>B</sub>*<sup>-</sup> *gal met*) were provided by L. Snyder (15). Originally, this T4 *alc* mutant was thought to carry the 4.2-kb rIIH23 deletion, but instead it has been found to carry a longer rII deletion, defined genetically as extending from or near the end

of the *rIIA* gene into the *ac* locus (8). We refer to this deletion as *rIIH23B*. By electron microscopy of heteroduplexes, we found that the *rIIH23B* deletion removes 5.8 kb and that its starting point at the end of the *rIIA* gene is indistinguishable from the starting point for the *rIIH23* deletion. Bacteriophage T2L and *E. coli* B were obtained from W. Harm.

**Growth of bacteriophage and isolation of DNA.** T4 *alc* quadruple-mutant particles that contained cytosine-containing DNA were grown by using first *E. coli* K803 and then *E. coli* B834, and the DNA was isolated by phenol extraction as described in the accompanying paper (9). T2L stocks were obtained by infection of exponentially growing *E. coli* B with single plaques; H broth was used as the medium; it contains (per liter) 8 g of nutrient broth (Difco Laboratories), 5 g of peptone (Difco), 5 g of NaCl, and 1 g of glucose. The T2L particles were purified by differential centrifugation and stored in 20 mM Tris-hydrochloride (pH 7.8)–0.5 mM EDTA.

**T2/T4 DNA hybridization.** T4 cytosine-containing DNA from the *alc* quadruple mutant was digested with *Bgl*II (New England Biolabs) as described in the accompanying paper (9) and then extracted with phenol. The mixture of T4 *Bgl*II fragments was hybridized with full-length T2 chromosomal strands essentially by the method of Davis et al. (4). This method minimizes breakage of the long chromosomal DNA strands by using alkali to simultaneously disrupt phage particles and denature the DNA in the same tube used for the hybridization. To  $5 \times 10^9$  T2 particles and 0.2  $\mu$ g of the T4 *Bgl*II fragments in 45  $\mu$ l, 5  $\mu$ l of 0.2 M EDTA (disodium salt)–1 M NaOH was added. After 10 min at room temperature, the solution was adjusted to pH 8.5 with 7  $\mu$ l of 1.5 M Tris-hydrochloride (pH 7.8)–0.2 M Tris base, and then 41 to 43  $\mu$ l of 99% formamide was added. Renaturation of the DNA was allowed to proceed at room temperature for 2 h during dialysis against a solution containing 0.45 M NaCl, 0.1 M Tris-hydrochloride (pH 8.5), 0.01 M EDTA, and 40 to 50% formamide or for 5 h without dialysis. The conditions were designed to permit 50% of the molecules to anneal.

**Electron microscopy.** Circular, single-stranded fd DNA (Miles Laboratories, Inc.) containing 6,408 nucleotides (1) and double-stranded pBR322 DNA (obtained from H. Boyer in *E. coli* RR1) containing 4,362 base pairs (bp) (16) were added to the T2/T4 hybrid molecules as internal length standards. The DNA was spread onto a monolayer of cytochrome *c* in the presence of formamide as described by Davis et al. (4) and then picked up on carbon-coated grids. The grids were rotary shadowed with Pt and photographed with a Siemens 1A electron microscope at  $\times 10,000$ . Lengths of DNA molecules were measured on projections of photographic negatives by using a linear integrator (Numonics Graphics).

## RESULTS

**T2/T4 *alc* mutant heteroduplex.** The use of nonhomology loops as markers to locate the ends of *Bgl*II fragments on the T2/T4 heteroduplex map, which in turn permitted an alignment of the restriction and genetic maps, re-

quired verification of the published wild-type T2/T4 heteroduplex map for the strains which we used. Because of their circular permutation, T2 and T4 form large circular heteroduplexes when denatured and reannealed. Measurements made on such heteroduplexes formed from T2L and the T4 *alc* quadruple-mutant chromosomal strands yielded a map of substitution and deletion loops (Fig. 1, outer circle) identical to the one constructed by Kim and Davidson (7) for wild-type DNAs, except for an additional substitution-type nonhomology labeled G', which we consistently observed, and a 5.8-kb deletion loop that resulted from the *rIIH23B* mutation carried by the T4 *alc* quadruple mutant. As pointed out by Kim and Davidson (7), this heteroduplex map is an idealized map. In individual heteroduplexes, neighboring loops sometimes merged to give a bigger loop. In other cases, large substitution loops underwent additional base pairing, creating several smaller loops; sometimes loops collapsed or became twisted and appeared as stretches of homologous DNA. For example, several smaller loops were often observed in place of the F loop, and the homologous regions between loops V' and U' or between loops H and S often remained unpaired, generating loops larger than normal.

**Heteroduplex mapping of the T4 *Bgl*II fragments.** The *Bgl*II restriction fragments from a total digestion of T4 *alc* mutant cytosine-containing DNA (Table 1) were hybridized with full-length T2 chromosome strands and examined by electron microscopy. Of 50 well-spread heteroduplex molecules which were chosen for measurement, one-half could be assigned to specific T4 *Bgl*II fragments. The others either could not be positioned unambiguously on the heteroduplex map on the basis of their loop patterns or did not correspond in length to one of the known *Bgl*II fragments. Some examples in this latter category were to be expected due to random cutting of the ends of T4 chromosomes during phage DNA packaging.

For the initial measurement of the length of the T4 DNA strand in a heteroduplex, the two arms of the substitution loops were averaged, and the lengths of the deletion loops were divided in half unless the loops were already assigned to T2 or T4 DNA by Kim and Davidson (7). In the case of *Bgl*II fragments 5 and 7a, once heteroduplexes were correlated with these fragments, the measured lengths of the T4 DNA strands were adjusted upward by assignment of previously unassigned single-stranded loops to T4 DNA in order to more exactly match the known lengths of these fragments.

Figure 2 shows examples of the heteroduplex molecules that could be correlated with *Bgl*II

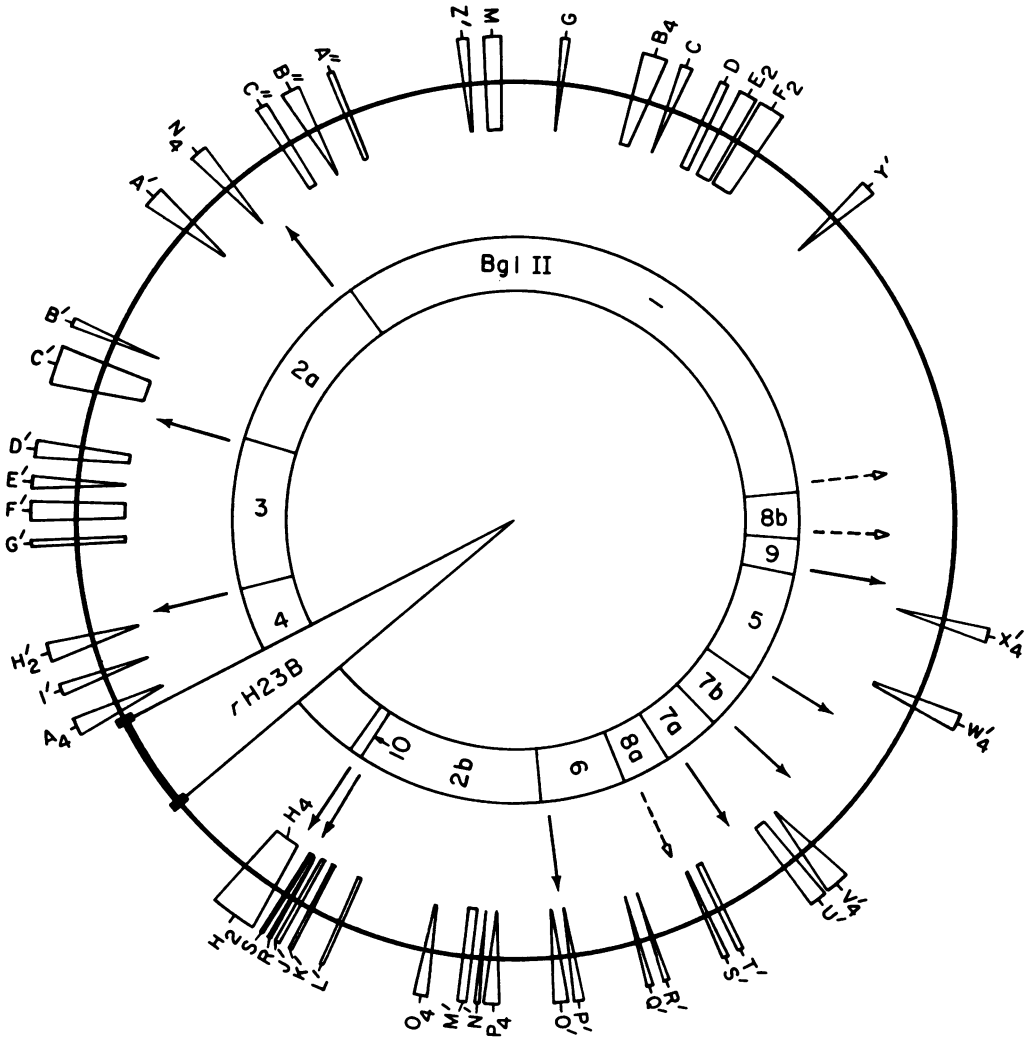


FIG. 1. *Bgl*II restriction map of T4 (inner circle) aligned with respect to the T2/T4 heteroduplex map (outer circle). The solid arrows indicate *Bgl*II cleavage sites located on the heteroduplex map by visualization of heteroduplexes formed between T4 *Bgl*II fragments and full-length T2 chromosomal strands. The dashed arrows indicate the *Bgl*II cleavage sites assigned to the heteroduplex map on the basis of their relative locations on the restriction map. The circular heteroduplex map was drawn by averaging the lengths of the two arms of substitution loops and taking one-half of the lengths of deletion loops. The letter designations given to some of the nonhomologies on the heteroduplex map by Kim and Davidson (7) have been retained; the remainder of the nonhomologies are designated with letters that carry primes. The subscripts 2 and 4 are used to indicate the sources of the single strands in the nonhomology loops, if known (T2 and T4, respectively). The full-length of the 5.8-kb *rIIH23B* deletion carried by the T4 *alc* mutant is represented as a segment bisecting both maps. Its boundaries were used to fix the alignment of the maps.

fragments 2a, 2b, 3, 4, 5, and 7a. Figure 3 shows the average lengths of the T4 DNA strands and of the individual duplex and single-stranded regions of all measured heteroduplexes. In the middle of the heteroduplex in Fig. 2a, a prominent deletion loop that corresponds in size to the 5.8-kb *rIIH23B* deletion is easily recognized. About 400 bp away is the neighboring deletion

loop A, which was assigned to T4 DNA by Kim and Davidson (7) because the duplex segments between loop A and various *rII* deletion loops often open up to form single substitution-type loops, the arms of which can be accounted for only if loop A is T4 DNA. Missing from the heteroduplex in Fig. 2a is loop I', which should be visible between loop A<sub>4</sub> and the left end of

TABLE 1. *Bgl*II fragments of T4 *alc* mutant cytosine-containing DNA

Fragment	Size (bp) <sup>a</sup>
1	55,840
2a	17,530
2b	17,500
3	14,010
4	12,660
5	10,580
6	7,940
7a	5,540
7b	5,470
8a	4,410
8b	4,350
9	3,330
10	1,180

<sup>a</sup> Sizes, as determined by agarose gel electrophoresis, were adjusted slightly by a least-squares analysis designed to yield a best-fit map for the fragments produced by *Bgl*II and five other restriction endonucleases (9).

the molecule. Apparently it collapsed in this example, which was chosen for illustration because base pairing of the segment between the rIIIH23B and A<sub>4</sub> loops had occurred and all other regions were well spread during mounting. In other examples of this heteroduplex, loop Y' was visible either as a deletion-type loop or as the asymmetric substitution-type loop shown in Fig. 3.

At each end of the heteroduplex region in Fig. 2a is a single-stranded tail of T4 DNA; the single-stranded T2 DNA extends over a much longer distance, past the edges of the micrograph. Cleavage of T4 *alc* DNA by *Bgl*II within the H nonhomology region would have generated the 1.32-kb tail of T4 DNA at the right end of the heteroduplex. How the tail of T4 DNA which was seen at the left end of all examples of this heteroduplex was generated is not directly apparent. It could have resulted from cleavage by *Bgl*II within the H' deletion loop, which was not assigned to T2 or T4 DNA (7). However, as an examination of the end of the heteroduplex formed with the adjoining *Bgl*II fragment showed (Fig. 2d and 3; see below), the H' loop was apparently T2 DNA, and cleavage of the T4 DNA occurred 560 bp beyond the H' deletion loop. Thus, the tail of T4 DNA appears to have resulted from a failure of the T4 DNA to base pair with T2 sequences beyond the H<sub>2</sub> loop, probably due to insufficient homology and the lack of a well-paired neighboring region, as would be found in a complete T2/T4 heteroduplex.

Altogether, the sequences assigned to T4 in the heteroduplex shown in Fig. 2a were 12.36 ± 0.09 kb long (Fig. 3), indicating that the T4 DNA strand was derived from *Bgl*II fragment 4, which

was 12.66 kb long, as determined by agarose gel electrophoresis.

On the *Bgl*II restriction map of the T4 *alc* mutant DNA, one end of *Bgl*II fragment 4 adjoins the smallest *Bgl*II fragment (fragment 10), and beyond that is fragment 2b. The heteroduplex that corresponds to this fragment is shown in Fig. 2b. It contains the seven nonhomology loops from K' to O', which extend from near the end of *Bgl*II fragment 4 in the H substitution loop in a counterclockwise direction. A small, eighth loop was present between M' and N', but it did not occur regularly in T2/T4 heteroduplexes and thus was not designated with a letter. Given the fact that deletion loops O and P represent T4 DNA (7), the T4 strand in this heteroduplex was 17.97 ± 0.21 kb long (Fig. 3), compared with 17.50 kb for *Bgl*II fragment 2b from agarose gels.

The right end of *Bgl*II fragment 2b was generated by cleavage 190 bp beyond loop O', within a region of T2/T4 homology. At the left end, cleavage occurred between loops S and R, leaving space for *Bgl*II fragment 10 between fragments 2b and 4 (Fig. 1). Note that in the heteroduplex shown in Fig. 2b the strand of T2 DNA terminated within the region of homology between loops K' and J', leaving the T4 DNA unpaired over the relatively short distance to the homology region between loops S and R.

Proceeding around the restriction map from *Bgl*II fragment 2b, the next fragments for which unambiguous heteroduplexes were observed were fragments 7a and 5, both of which are shown hybridized to the same T2 DNA strand in Fig. 2c. The intervening fragment 7b is absent, and except for this particular example, its corresponding sequence along the T2 DNA would have remained undetected, as it contains no observable nonhomologies. In agarose gels, fragment 7b was 5.47 kb long; in Fig. 2c the corresponding T2 single-stranded region was 5.39 kb long.

The region to which *Bgl*II fragment 7a was hybridized covered deletion loop V' and substitution loop U'. The 1.39-kb loop V' was not assigned to either T2 or T4 by Kim and Davidson, but must be T4 DNA if the measured length of the T4 strand in the heteroduplex is to match the length of *Bgl*II fragment 7a. Including V', the T4 fragment was 5.76 kb long (Fig. 3); in agarose gels, fragment 7a was 5.54 kb long. The counterclockwise end of fragment 7a could be placed 1.85 kb beyond loop V'. The other end was located about 1 kb past the U' substitution loop in a region which normally is base paired in full-length T2/T4 hybrids but remained unpaired in this heteroduplex.

*Bgl*II fragment 5 was 10.58 kb long as deter-

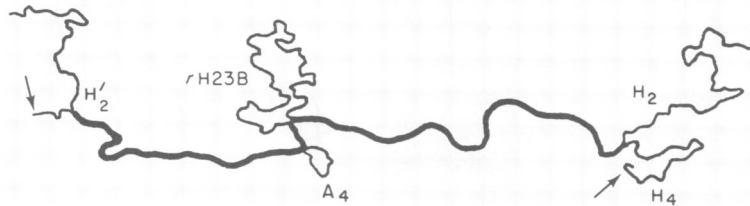
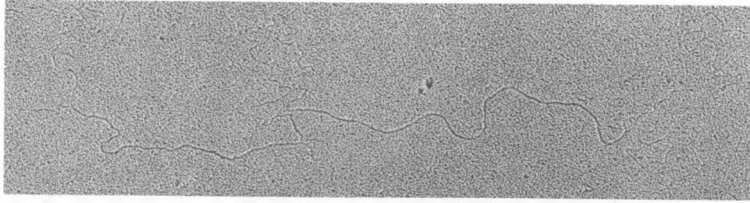
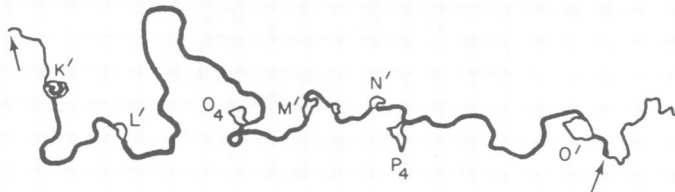
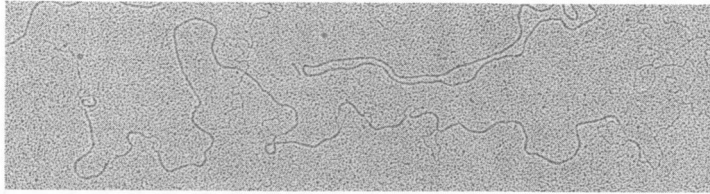
a) T2/T4 *Bgl*II fragment 4b) T2/T4 *Bgl*II fragment 2b

FIG. 2. Electron micrographs and tracings of heteroduplex DNAs formed from full-length T2 chromosomal strands and strands from *Bgl*II fragments of T4. The arrows designate the ends of the T4 DNA strands and, thus, *Bgl*II cleavage sites. Nonhomology loops are designated by letters as described in the legend to Fig. 1.

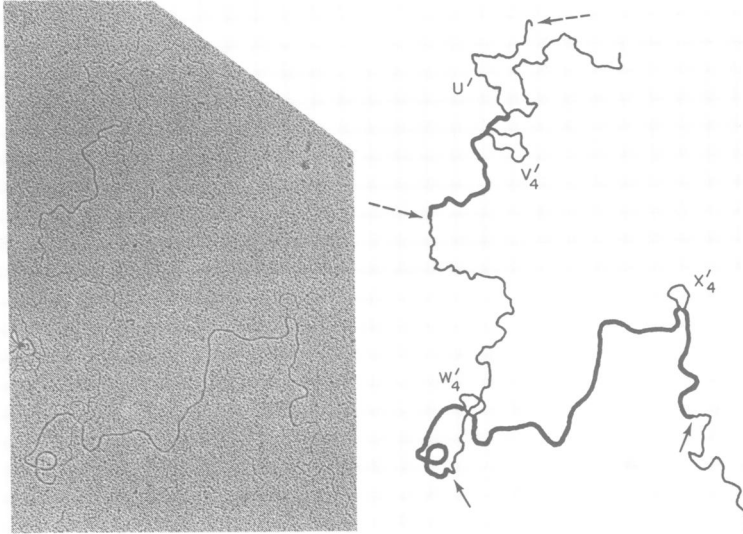
mined by agarose gels. To account for this length in the corresponding heteroduplex in Fig. 2c, we assigned the long arm of substitution loop W' and the deletion loop X' to T4. Altogether, the T4 strand in the heteroduplex then was  $10.42 \pm 0.42$  kb long (Fig. 3). *Bgl*II cleavage sites were located 2.47 kb before loop W', and 1.85 kb after loop X'.

Turning to the restriction fragments located on the clockwise side of *Bgl*II fragment 4, examples of the heteroduplexes assigned to fragments 3 and 2a are shown in Fig. 2d and e, respectively. The heteroduplex in Fig. 2d contained the readily recognized pattern of non-homologies between loops D' and G' and contained a T4 strand with an average length of  $14.12 \pm 0.13$  kb (Fig. 3). From agarose gels, *Bgl*II

fragment 3 was 14.01 kb long. Note that the right end of the heteroduplex region which adjoined fragment 4 was fully duplex and, according to its 6.02-kb distance from loop G', terminated before the H' deletion loop, which was 6.23 kb from loop G'. This supports the earlier assignments of loop H' to T2 DNA and the *Bgl*II cleavage site at the end of fragment 4 to the homologous region beside the H' loop rather than to the DNA within the H' loop. However, our assignment of loop H' to T2 DNA can only be tentative. The left end of the heteroduplex with *Bgl*II fragment 3 is located 2.80 kb from loop D'.

The heteroduplex in Fig. 2e contained the nonhomologies C' through N', along with an unlettered substitution loop near N', which was

c) T2/T4 *Bg*/II fragments 5 and 7a



d) T2/T4 *Bg*/II fragment 3

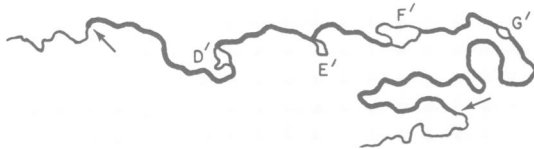
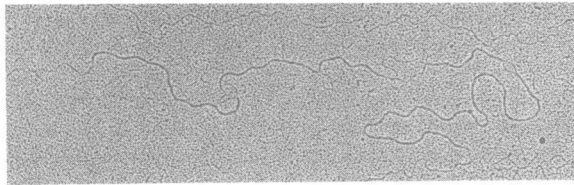


**FIG. 2 c and d.**

e) T2/T4 *Bg*/II fragment 2a

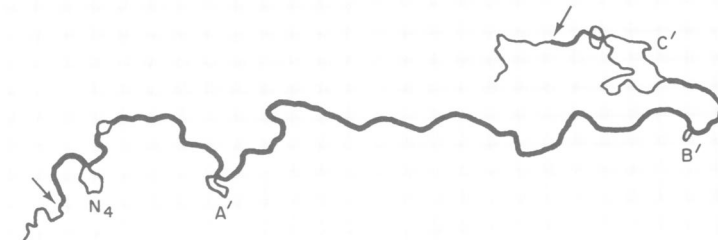
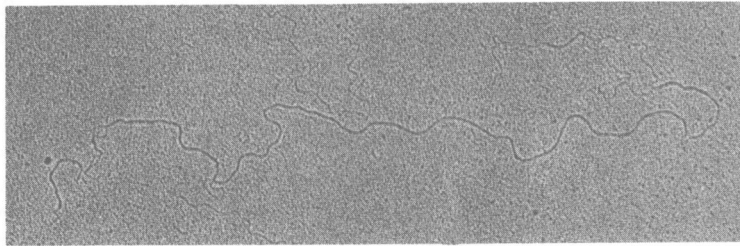


**FIG. 2 e.**

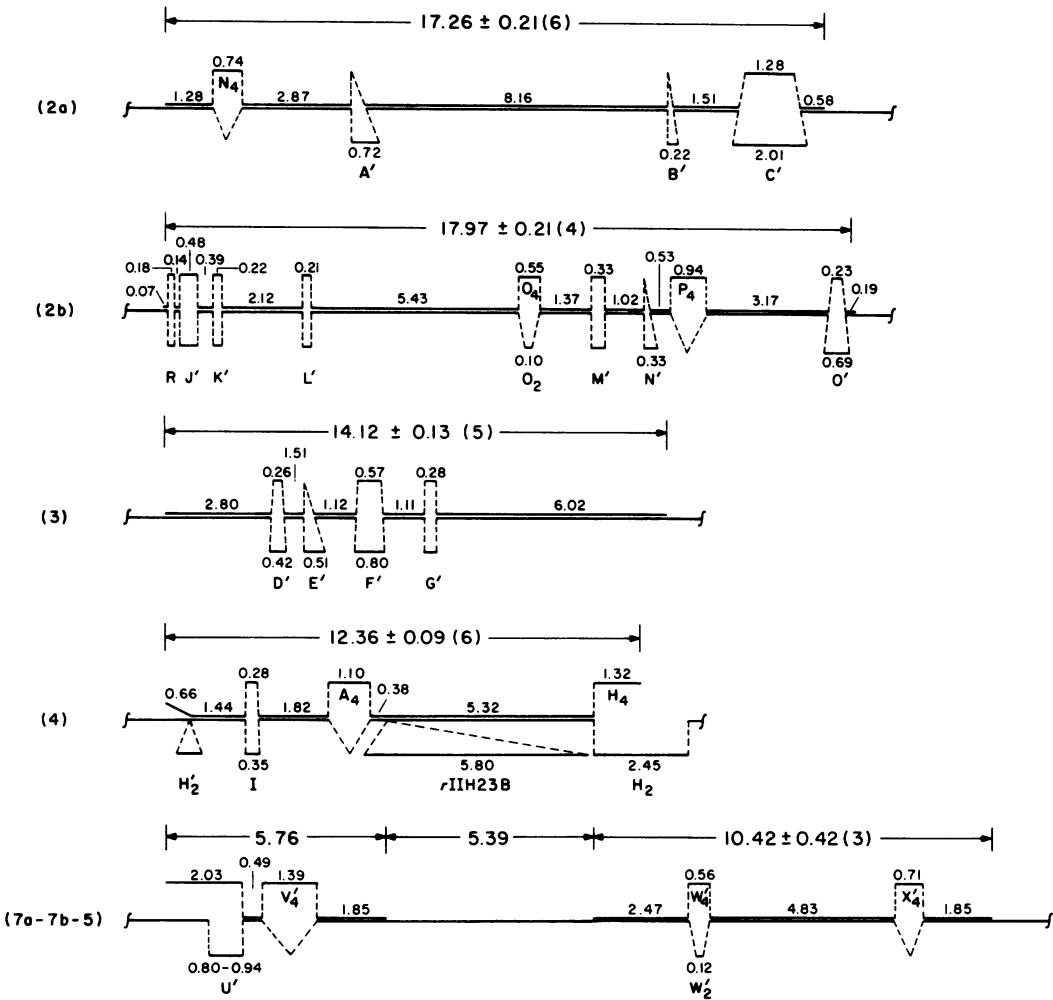


FIG. 3. Maps of the T2/T4 *Bgl*III fragment heteroduplexes. The heteroduplexes are numbered according to the T4 *Bgl*III fragment which they contain. Distances are given in kilobases for each duplex and single-stranded region. The average length  $\pm$  standard deviation for each T4 strand is given above each map, and the number of heteroduplexes measured is given in parentheses. The two values given for the length of substitution loop U' in the heteroduplex with *Bgl*III fragment 7a represent the lengths of the two arms of the loop in full T2/T4 heteroduplexes. Here the upper arm is not shown due to the lack of base pairing beyond the loop in the heteroduplex with the *Bgl*III fragment.

only occasionally observed and is not shown in Fig. 3. The average length of the T4 strand was  $17.26 \pm 0.21$  kb, compared with a value of 17.53 kb for *Bgl*III fragment 2a measured with agarose gels. The right end of the heteroduplex region terminated 580 bp beyond loop C'. This was within 60 bp of the location assigned to the same *Bgl*III cleavage site by measuring from loop D' in the heteroduplex with *Bgl*III fragment 3. The left end of the heteroduplex with *Bgl*III fragment 2a was located 1.28 kb before loop N<sub>4</sub>, within 170 bp of the location assigned to this *Bgl*III cleavage site by measuring from loop C'' in heteroduplexes formed with part of the neighboring *Bgl*III

fragment 1 (data not shown). Several heteroduplexes containing this end of *Bgl*III fragment 1 were found, although no unambiguous heteroduplexes containing the entire 56-kb *Bgl*III fragment were observed.

**Alignment of the T4 restriction and genetic maps.** Altogether, the heteroduplexes between T2 DNA and the T4 *Bgl*III fragments permitted 10 of the 13 *Bgl*III cleavage sites on the T4 *alc* mutant DNA to be located on the T2/T4 heteroduplex map. The exact location of the large rIIH23B deletion on the T2/T4 heteroduplex map and within *Bgl*III fragment 4 was also defined. By using this deletion as a point of

reference and the *Bgl*III cleavage sites to correctly orient the T4 *Bgl*III restriction map with respect to the T2/T4 heteroduplex map, the two maps were aligned, as shown in Fig. 1. The small differences observed between the locations of the cleavage sites on the restriction map (Fig. 1, inner circle) and the locations of the cleavage sites on the heteroduplex map (Fig. 1, arrows pointing toward the outer circle) reflect the fact that the restriction map is a strictly physical map of the T4 genome, whereas the heteroduplex map was constructed by averaging the lengths of the substitution loop arms and halving the lengths of the deletion loops. This procedure was necessary because not all loops could be assigned to T2 or T4. Over long distances, the contributions from T2 and T4 average out, but over short distances, unequal amounts of DNA attributable to T2 or T4 can cause the *Bgl*III sites on the heteroduplex map to be shifted relative to the physical restriction map.

As Fig. 1 shows, two of the three *Bgl*III cleavage sites not directly located by the heteroduplex analysis fall at the ends of fragments that contain no nonhomology loops, i.e., fragments 8b and 9. These two neighboring sites could be located on the T2/T4 heteroduplex map by measuring from the *Bgl*III cleavage site located between fragments 5 and 9. The last *Bgl*III site falls between fragments 8a and 6. Its location on the heteroduplex map could not be determined exactly due to the presence of unassigned deletion loops in both of these fragments; however, by measuring from the *Bgl*III cleavage site at the end of fragment 7a, it could be defined as lying at one end or the other of a 330-bp interval, which is a distance equal to the unassigned S' deletion loop in fragment 8a.

The final alignment of the *Bgl*III restriction map with the T4 genetic map is shown in Fig. 4. Also included are the cleavage sites for the five other restriction enzymes mapped in the accompanying report (9). The alignment is based on the prior orientation of the T2/T4 heteroduplex map with the T4 genetic map as described by Kim and Davidson (7). The *r*II locus was used as the primary reference point for the alignment, with the start of the *r*IIH23B deletion being placed at the left end of the *r*IIA gene. The *r*IIA gene has been estimated to contain 2,300 bp by electron microscopy of heteroduplexes formed with various *r*II deletion mutants (7). This is in line with length estimates based on the molecular weight of the *r*IIA protein (13).

## DISCUSSION

*Bgl*III cleaves the cytosine-containing DNA of T4 *amE51 nd28 r*IIH23B *alc8* into 13 fragments,

6 of which we have identified in heteroduplexes with full-length T2 chromosomal strands. The ends of these heteroduplexes specified the locations of 10 of the *Bgl*III cleavage sites on the T2/T4 heteroduplex map, providing the framework for (i) the assignment of the remaining 3 *Bgl*III cleavage sites on the heteroduplex map, (ii) the identification of the source of DNA in four more of the nonhomology loops on the T2/T4 heteroduplex map, and (iii) the orientation of the restriction map with respect to the T4 genetic map. The final alignment between the restriction and genetic maps was fixed by the location of the start of the *r*IIH23B deletion at the end of the *r*IIA gene.

The accuracy with which the ends of the T4 DNA strands in the heteroduplexes with T2 could be identified, and thus the accuracy with which the *Bgl*III restriction sites could be assigned to the T2/T4 heteroduplex map, can be gauged by examining those cases where heteroduplexes were found for neighboring restriction fragments (e.g., fragments 1 and 2a or fragments 2a and 3). In these two cases, the independent assignment of the restriction sites varied by only 60 and 170 nucleotide pairs. This is in line with the limit of resolution expected for heteroduplex mapping by electron microscopy.

Because our alignment of the T4 restriction map with the genetic map is fixed at the *r*II locus, its accuracy over the entirety of the map depends upon the extent to which the genetic map itself represents true physical distances along the DNA. Actually, the correlation should be quite good, as the genetic map in Fig. 3 is not a classical map based only on recombination frequencies, which can vary from region to region within the genome. For many loci, the genetic map represents physical distances determined by measuring the frequency with which two given genes are carried together on the incomplete chromosomes found in small T4 particles (10, 11). The positions of the remaining genes were interpolated from recombination frequencies. The distance in kilobase pairs between the *r*II and lysozyme genes was measured directly by electron microscopy of deletion heteroduplexes (7). These two loci are nearly opposite one another on the circular genetic map and thus have served to fix distances along the T4 genetic map at two widely separated points. Between these points some distortion can be anticipated, but it should not be too great.

The location of the single *Bam*HI cleavage site can be taken as an indication of the degree with which the restriction and genetic maps coincide outside the *r*II and lysozyme regions. Our alignment places the *Bam*HI site within gene 8, very near its juncture with gene 7. This





*Bgl*II, *Kpn*I, and *Sal*I cleavage patterns of several T4 deletion mutants to determine a general alignment between the maps. O'Farrell et al. (12) have constructed a T4 restriction map which contains the *Eco*RI, *Hind*III, and *Pst*I cleavage sites and have aligned it with the T4 genetic map by hybridization of restriction fragments to cloned segments of the T4 genome and by correlation of restriction fragment sizes with the pattern of fragments produced by digestion of the cloned DNAs. In both cases, there was agreement with the alignment which we found for the restriction and genetic maps.

#### ACKNOWLEDGMENTS

This investigation was supported by Public Health Service research grant GM 23608 from the National Institute of General Medical Sciences and by Public Health Service Research Career Development Award CA 00490 to R.C.M. from the National Cancer Institute.

#### LITERATURE CITED

1. Beck, E., R. Sommer, E. A. Auerswald, C. Kurz, B. Zink, C. Osterburg, H. Schaller, K. Sugimoto, H. Sugisaki, T. Okamoto, and M. Takanami. 1978. Nucleotide sequence of bacteriophage fd DNA. *Nucleic Acids Res.* **5**:4495-4503.
2. Carlson, K. 1980. Correlation between genetic map and map of cleavage sites for sequence-specific endonucleases *Sal*I, *Kpn*I, *Bgl*II, and *Bam*HI in bacteriophage T4 cytosine-containing DNA. *J. Virol.* **36**:1-17.
3. Carlson, K., and B. Nicolaisen. 1979. Cleavage map of bacteriophage T4 cytosine-containing DNA by sequence-specific endonucleases *Sal*I and *Kpn*I. *J. Virol.* **31**:112-123.
4. Davis, R. W., M. Simon, and N. Davidson. 1971. Electron microscope heteroduplex methods for mapping regions of base sequence homology in nucleic acids. *Methods Enzymol.* **21D**:413-428.
5. Hänggi, U. J., and H. G. Zachau. 1980. Isolation and characterization of DNA fragments containing the dihydrofolate-reductase gene of coliphage T4. *Gene* **9**:271-285.
6. Kiko, H., E. Niggemann, and W. Rüger. 1979. Physical mapping of the restriction fragments obtained from bacteriophage T4 dC-DNA with restriction endonucleases *Sma*I, *Kpn*I and *Bgl*III. *Mol. Gen. Genet.* **172**:303-312.
7. Kim, J.-S., and N. Davidson. 1974. Electron microscope heteroduplex study of sequence relations of T2, T4, and T6 bacteriophage DNAs. *Virology* **57**:93-111.
8. Kutter, E., A. Beug, R. Sluss, L. Jensen, and D. Bradley. 1975. The production of undegraded cytosine-containing DNA by bacteriophage T4 in the absence of dCTPase and endonucleases II and IV, and its effect on T4-directed protein synthesis. *J. Mol. Biol.* **99**:591-607.
9. Marsh, R. C., and M. L. Hepburn. 1981. Map of restriction sites on bacteriophage T4 cytosine-containing DNA for endonucleases *Bam*HI, *Bgl*II, *Kpn*I, *Pvu*I, *Sal*I, and *Xba*I. *J. Virol.* **38**:104-114.
10. Mosig, G. 1968. A map of distances along the DNA molecule of phage T4. *Genetics* **59**:137-151.
11. Mosig, G. 1976. Linkage map and genes of bacteriophage T4, p. 664-676. In G. D. Fasman (ed.), *Handbook of biochemistry and molecular biology*, 3rd ed. Nucleic acids, vol. 2. CRC Press, Cleveland, Ohio.
12. O'Farrell, P., E. Kutter, and M. Nakanishi. 1980. A restriction map of the bacteriophage T4 genome. *Mol. Gen. Genet.* **179**:421-435.
13. O'Farrell, P. Z., L. M. Gold, and W. M. Huang. 1973. The identification of prereplicative bacteriophage T4 proteins. *J. Biol. Chem.* **248**:5499-5501.
14. Rüger, W., M. Neumann, U. Rohr, and E. Niggemann. 1979. The complete maps of *Bgl*II, *Sal*I and *Xho*I restriction sites on T4 dC-DNA. *Mol. Gen. Genet.* **176**:417-425.
15. Snyder, L., L. Gold, and E. Kutter. 1976. A gene of bacteriophage T4 whose product prevents true late transcription on cytosine-containing T4 DNA. *Proc. Natl. Acad. Sci. U.S.A.* **73**:3098-3102.
16. Sutcliffe, J. G. 1979. Complete nucleotide sequence of the *Escherichia coli* plasmid pBR322. Cold Spring Harbor Symp. Quant. Biol. **43**:77-90.
17. Wilson, G. G., R. L. Neve, G. J. Edlin, and W. H. Konigsberg. 1979. The *Bam* HI restriction site in the bacteriophage T4 chromosome is located in or near gene 8. *Genetics* **93**:285-296.
18. Wood, W. B., and H. R. Revel. 1976. The genome of bacteriophage T4. *Bacteriol. Rev.* **40**:847-868.